JACS
JOURNAL OF THE AMERICAN CHEMICAL SOCIETY

Article

pubs.acs.org/JACS

Hierarchical N-Doped Carbon as CO_2 Adsorbent with High CO_2 Selectivity from Rationally Designed Polypyrrole Precursor

John W. F. To,[†,⊥] Jiajun He,[‡,⊥] Jianguo Mei,[†,§] Reza Haghpanah,[‡] Zheng Chen,[†] Tadanori Kurosawa,[†] Shucheng Chen,[†] Won-Gyu Bae,[†] Lijia Pan,[∥] Jeffrey B.-H. Tok,[†] Jennifer Wilcox,[*,‡] and Zhenan Bao[*,†]

[†]Department of Chemical Engineering and [‡]Department of Energy Resources Engineering, Stanford University, Stanford, California 94305, United States

[§]Department of Chemistry, Purdue University, West Lafayette, Indiana 47907, United States

[∥]Collaborative Innovation Center of Advanced Microstructures, Jiangsu Provincial Key Laboratory of Photonic and Electronic Materials, School of Electronic Science and Engineering, Nanjing University, Nanjing 210093, China

Supporting Information

ABSTRACT: Carbon capture and sequestration from point sources is an important component in the CO_2 emission mitigation portfolio. In particular, sorbents with both high capacity and selectivity are required for reducing the cost of carbon capture. Although physisorbents have the advantage of low energy consumption for regeneration, it remains a challenge to obtain both high capacity and sufficient CO_2/N_2 selectivity at the same time. Here, we report the controlled synthesis of a novel N-doped hierarchical carbon that exhibits record-high Henry's law CO_2/N_2 selectivity among physisorptive carbons while having a high CO_2 adsorption capacity. Specifically, our synthesis involves the rational design of a modified pyrrole molecule that can co-assemble with the soft Pluronic template via hydrogen bonding and electrostatic interactions to give rise to mesopores followed by carbonization. The low-temperature carbonization and activation processes allow for the development of ultrasmall pores (d < 0.5 nm) and preservation of nitrogen moieties, essential for enhanced CO_2 affinity. Furthermore, our described work provides a strategy to initiate developments of rationally designed porous conjugated polymer structures and carbon-based materials for various potential applications.

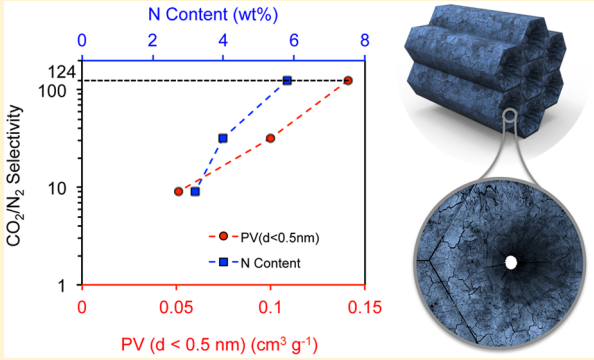

INTRODUCTION

The mitigation of carbon dioxide (CO_2) emissions has been recognized as a crucial necessity, due to its effects toward global warming and associated consequences.[1] Porous carbons have gained continuous interest due to their broad range of applications in CO_2 capture,[2,3] energy storage,[4] and catalysis.[5] For CO_2 capture, they possess a number of advantages, such as relatively low regeneration energy,[3,6] high surface area,[7] chemical stability, tunability over pore geometries, pore dimensions,[8,9] as well as flexibility for heteroatom doping or surface functionalization.[10] However, the major drawback of physisorptive carbons is their low CO_2/N_2 selectivity, which has hindered their applications at scale.[3,6]

An especially appealing approach toward enhancing sorbent's CO_2 selectivity is to carefully tune the ultramicropore size to enhance adsorption potential energy. Nugent et al. have demonstrated this concept on a metal−organic framework (MOF) to achieve optimal adsorption thermodynamics and hence high CO_2 selectivity.[11] An ideal sorbent should possess a hierarchical structure, in which the ultramicropores will provide high selectivity and capacity, while the mesopores are important for allowing fast gas diffusion. However, such hierarchical structures remain to be challenging to rationally design and synthesize in carbon-based sorbents. Extensive works have been carried out on the synthesis of mesoporous carbon through the interfacial assembly from organic prepolymers of phenolic resol.[12−18] Here we extend the synthetic approach for the first time to the formation of ordered mesoporous conjugated polymer-based carbon. Our porous carbon was prepared using low-temperature carbonization (≤500 °C) of a rigid conjugated polymer organic framework (Poly-OF) synthesized through co-assembly and polymerization of a rationally designed pyrrole monomer and a triblock copolymer soft-template. Ultramicropores are generated due to the cleavage of the carboxylic acid groups on the pyrrole monomer, which is also required for the co-assembly process. The low-temperature carbonization and activation processes allow controllability over the ultramicropore volume and nitrogen functional groups, which are essential for CO_2 adsorption under postcombustion conditions. The final product through this controlled synthetic approach demonstrates high CO_2 adsorption capacity (4.5 mmol g^{-1} at

Received: November 18, 2015
Published: December 30, 2015

DOI: 10.1021/jacs.5b11955
J. Am. Chem. Soc. 2016, 138, 1001−1009

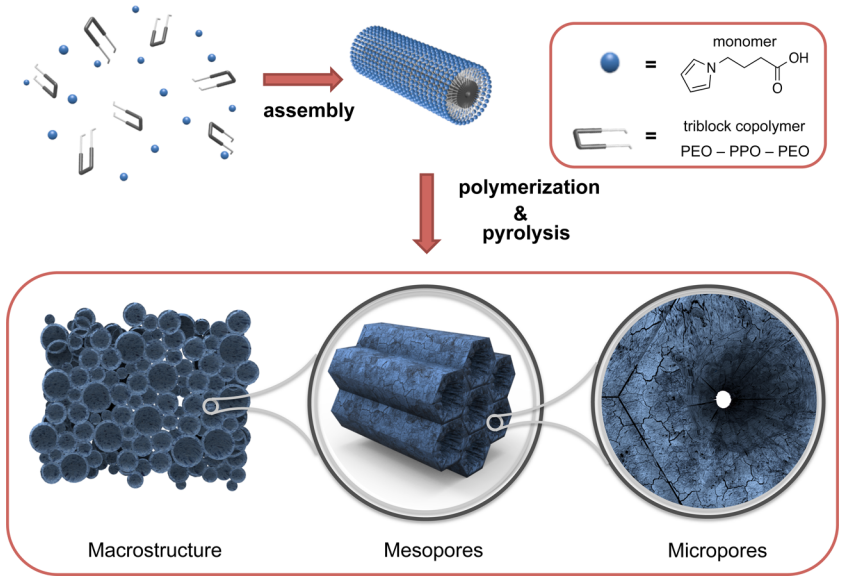

Figure 1. Schematic illustration of the synthesis and the hierarchical porous structures of the SU-MAC materials. 4-(1H-pyrrol-1-yl)butanoic acid and triblock copolymer, Pluronic P-123, co-assemble into a mesostructure, which is then polymerized and carbonized. The formation of hollow sphere structures is a result of tuning electrostatic interactions through adjusting solution pH during co-assembly process. The mesopores are formed upon removal of the soft triblock copolymer template, while the micropores are from cleavage of carboxylic groups and interdiffusion of the triblock copolymer into polypyrrole. The resulting carbon possesses hierarchical pore structure with macro-, meso-, and micropores.

298 K and 1 bar), mild regeneration conditions, reversible cyclability, and excellent stability under humid or acid operating conditions, and more importantly, our developed material is observed to possess record-high Henry's law CO_2/N_2 selectivity (124:1 at 298 K; 194:1 at 323 K) among physisorptive carbon materials while possessing high adsorption capacity. Such a combination of desirable features is required for practical sorbent applications at scale. In particular, a relatively high selectivity potentially leads to enhanced purity of the CO_2 in the enriched product stream in pressure/vacuum swing adsorption (P/VSA) processes and hence a reduced capture cost, although rigorous process optimization is required for detailed cost analysis.[19] Furthermore, this work demonstrated the CO_2 capacity under acidic gas conditions relevant to postcombustion capture, which is the first time performed on nitrogen-doped physisorptive carbons. With the concept of such molecular design, this work would give insight into the synthesis of a new class of mesoporous conjugated polymers and their derived carbons, which would benefit applications over a wide range of interests.

RESULTS AND DISCUSSION

Synthesis of Hierarchical Carbon Sorbent. The design principle of our hierarchical carbon sorbent is to facilitate efficient gas diffusion due to its range of pore sizes and hierarchical pore structure.[20] Such a hierarchical structure is desirable for CO_2 capture, since the macroscopic networks facilitate CO_2 diffusion by reducing the mass-transfer resistance, while the ultramicropores are beneficial for CO_2 adsorption;[21,22] however, these structures are challenging to synthesize. Our strategy is to prepare such hierarchical structures via co-assembly of a rational design of the polymer monomer precursor with a triblock copolymer through soft templating. A schematic showing the synthesis process and the resulting hierarchical porous structures of the porous carbon is given in Figure 1.

To synthesize the hierarchical porous carbon, first, our monomer needs to be sufficiently hydrophilic so that it preferentially co-assembles with the hydrophilic part of the triblock copolymer surfactant template, but still has a hydrophobic component such that it can participate in the co-assembly process and not be left primarily to the aqueous phase.[8,23] In addition, it should not be too hydrophobic such that it prefers to assemble into the hydrophobic cores of the triblock copolymer micelles. For example, the unmodified pyrrole monomer was observed to assemble into the hydrophobic core, and this resulted in solid (instead of hollow) polypyrrole nanosphere particles. To meet all the above requirements, the 4-(pyrrol-1-yl)butanoic acid (Py-COOH) monomer was designed and synthesized. This monomer was observed to exhibit all our needed properties for the assembly process. More specifically, it was observed that its hydrophilic tail renders it partially soluble in water such that it can burrow itself into the palisade region of the micelles, yet avoiding being totally assimilated into the hydrophobic core (Figure 1). Previously, various polyaniline and polypyrrole nanostructures have been reported, and numerous applications have been made possible due to the intrinsic conductivity of conjugated polymers.[4,24] However, ordered mesoporous conducting polymer structure has not been achieved using soft templating method.

Macroporous structures of our sample are formed through tuning the electrostatic interaction by pH and microphase separation during the formation of porous polymer networks.[25] This strategy has previously been used to prepare various conducting polymer structures.[26] The mesoporous structures were generated by the structural directing triblock copolymer micelles, which are subsequently removed to give rise to mesopores. Finally, the micropores are created through the removal of the interpenetrating block copolymer tails into the polymer matrix and partly from the cleavage of the butanoic acid group.[27] The polymer composite was subject to a first heating treatment at a temperature of 350 °C to slowly

DOI: 10.1021/jacs.5b11955
J. Am. Chem. Soc. 2016, 138, 1001−1009

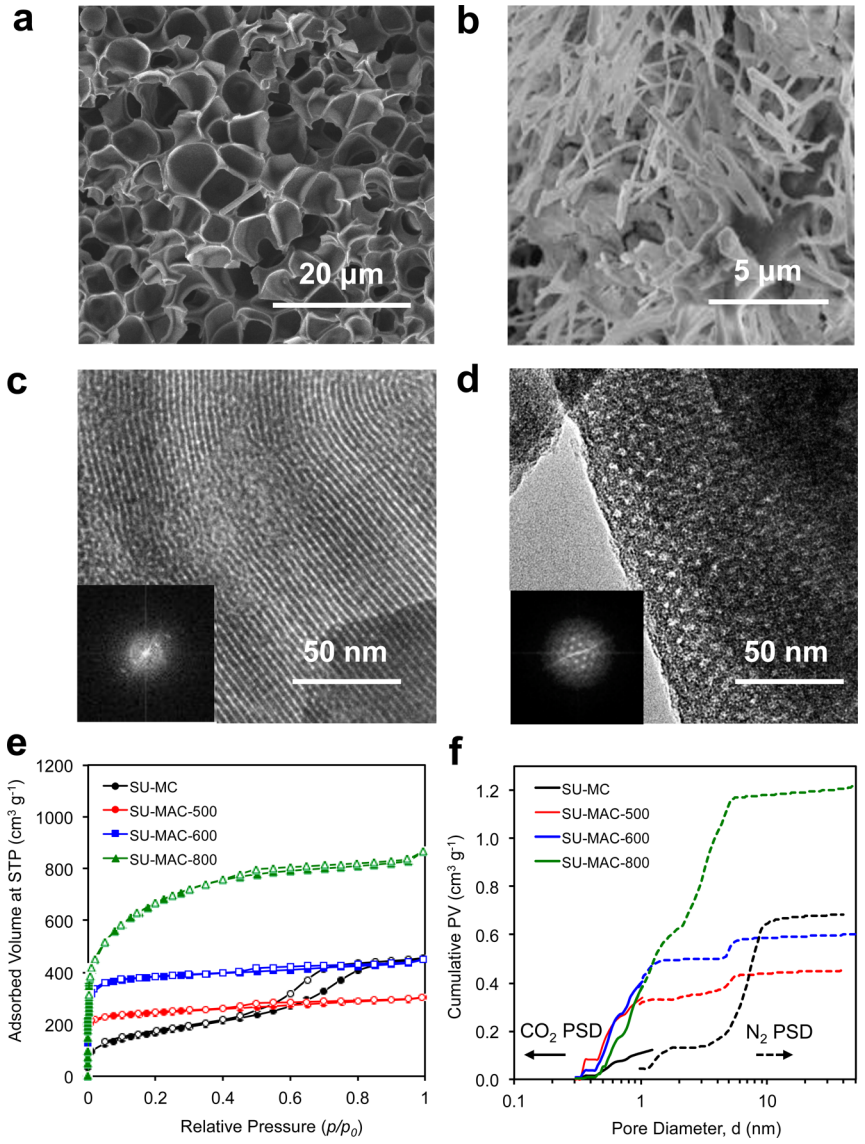

Figure 2. Morphological characterizations of the hierarchical carbons. (a, b) SEM images of SU-MC synthesized at pH = 2 and 3.5, respectively. (c, d) TEM of SU-MC showing the [110] and the [001] directions of the hexagonal array, respectively (insets: fast Fourier diffractograms). (e) N_2 adsorption (solid symbols) and desorption (open symbols) at 77 K for the SU-MC and SU-MAC samples. The total pore volumes were found to be 0.71, 0.47, 0.70, and 1.34 $cm^3\ g^{-1}$ for SU-MC, SU-MAC-500, SU-MAC-600 and SU-MAC-800, respectively. (f) Cumulative pore volumes of the SU-AC and SU-MAC samples, where the solid and broken lines represent the results from the CO_2 (273 K) and N_2 (77 K) adsorption tests, respectively.

decompose the triblock copolymer surfactant and carbonize the polypyrrole, denoted as nitrogen-doped mesoporous carbon (SU-MC). Thermogravimetric analysis (TGA) was performed on the as-synthesized polymer with a 5 °C min^{-1} rate, with a major decomposition between 350 and 400 °C, which corresponds to the removal of surfactant template (Figure S1). With increasing temperature from 500 to 800 °C, nitrogen moieties would convert to the more thermodynamically stable products, while the pore volume and surface area would increase due to rearrangement of the carbon layers to a more orderly structure and pore widening. In order to further improve the textural properties, a subsequent chemical activation using potassium hydroxide (KOH) at 500, 600, and 800 °C yields a series of nitrogen-doped hierarchical activated carbons, denoted as SU-MAC-500, 600 and 800, respectively. In addition, a different type of Pluronic surfactant has also been utilized for the tuning of pore size distribution and specific surface area (Figure S3). This shows that the as-designed monomer can co-assemble with different types of soft-templates. The approach in this work provides insights into the development of a new class of hierarchical porous materials via molecular engineering.

Structural Characterization of Hierarchical Carbon Sorbent. Scanning electron microscopy (SEM) images of the carbonized SU-MC samples (Figure 2a) show macroporous features of the carbon framework synthesized at pH = 2. This structure shows thin walls with interconnected void space. Interestingly, we also observed that the morphologies of the macroporous structures can be easily tuned by controlling the degree of protonation. By maintaining the pH at 1 or 3.5, either foam-like structures (Figure S4) or fiber-like structures are obtained (Figure 2b), respectively. A possible reason for the difference in obtained structures may be due to variations in the intra- and intermolecular electrostatic interactions affecting the

DOI: 10.1021/jacs.5b11955
J. Am. Chem. Soc. 2016, 138, 1001−1009

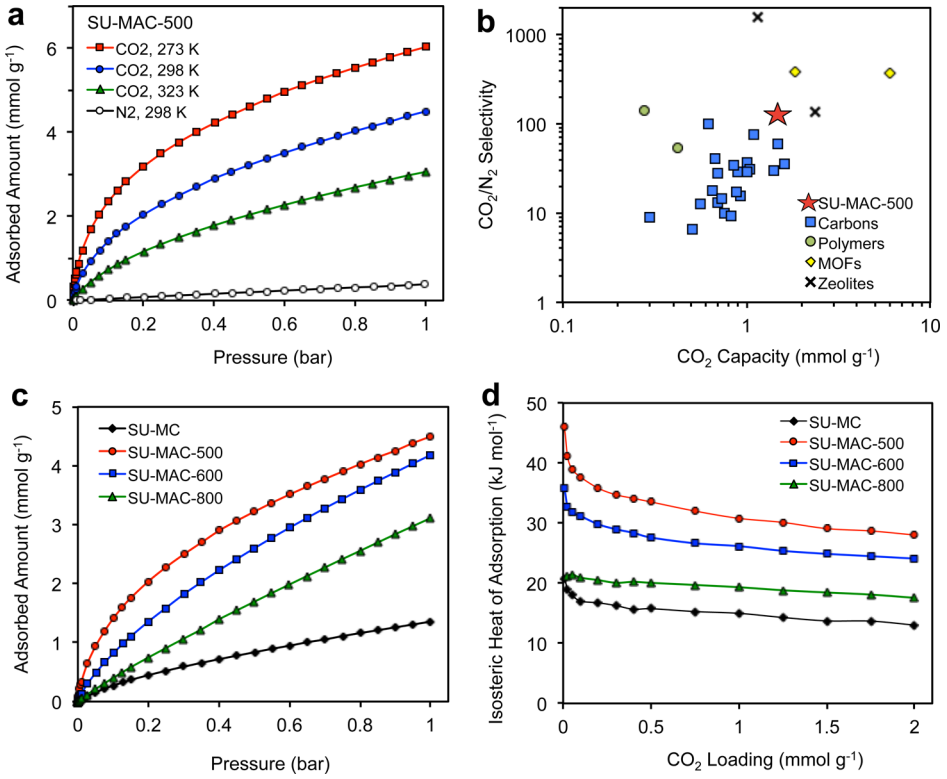

Figure 3. Gas-adsorption performance of SU-MAC carbons. (a) Gas adsorption performance of SU-MAC-500: CO_2 at 273, 298, and 323 K and N_2 at 298 K. (b) Comparison of CO_2 capacity (298 K, 0.1 bar) and Henry's law CO_2/N_2 selectivity of SU-MAC-500 with different types of solid physisorbents, with two representative high-selectivity materials selected for polymers,[31,36] MOFs,[37] and zeolites,[37] respectively (refer to Table S2 for a summary of carbon physisorptive materials). The carbon materials surveyed in this figure include N-doped carbons and other carbon physisorbents with highest reported selectivity. The Henry's law selectivities of MOFs and zeolites were taken from the low-pressure values based upon the IAST,[37] which converge to the Henry's law selectivities.[32] Note that although JBW (zeolite) shows the highest selectivity of ~1500, its low CO_2 capacity limits its use in a pressure swing adsorption (PSA) unit.[37] In addition, Mg-MOF-74 (MOF), albeit with high selectivity and capacity, is highly unstable when exposed to moisture,[38] hence limiting its practical applications.[38] (c) CO_2 adsorption isotherms at 298 K for the SU-MC and SU-MAC samples. (d) Isosteric heat of adsorption (Q_{st}) calculated using the Clausius−Clapeyron equation, based upon the CO_2 adsorption isotherms at 273, 298, and 323 K.

macrostructures formed from assembly of the polymer/soft-template nanostructures.[26] Previously, Stejskal et al. observed various polyaniline morphologies at different pHs due to different degrees of stabilization from hydrogen bonding and ionic interactions.[28] Liao et al. also showed that protonated pyrrole monomers formed cations which self-assembled with other anions and oxidants to form different polypyrrole nanostructures.[25]

Transmission electron microscopic (TEM) images and the corresponding Fourier diffractograms (Figure 2c,d) revealed a high degree of periodicity viewed from [110] and [001] directions, confirming the presence of two-dimensional hexagonal mesoporous structures. The periodicity of SU-MC was further confirmed using small-angle X-ray diffraction (XRD), as shown in Figure S5. The existence of the (100) and (200) peaks is clearly observed, which further supports the presence of two-dimensional hexagonal arrays.[17] The ordered mesoporous characteristics of the carbon could not have been achieved without the careful design and the molecular engineering of the monomer.

The nitrogen sorption isotherms (77 K) of SU-MC show remarkable hysteresis at $p/p_0 > 0.4$ (Figure 2e), corresponding to the major mesopore distribution centered at 6−8 nm (Figure 2f). The mesopores stem from the removal of the block copolymer template.[17] SU-MC also has 0.13 $cm^3\ g^{-1}$ of microporosity (d < 2 nm, Figure 2f), which originates from the cleavage of the butanoic acid side chain of the monomer. To tune the pore size distribution, i.e., micropore distribution, chemical activation was carried out on SU-MC using KOH as activating agent. A series of hierarchical carbons (SU-MAC-500, 600 and 800) with different micropore size distributions were synthesized by simply varying the activation temperature. The nitrogen sorption isotherms (77 K) (Figure 2e) of the three SU-MAC samples all showed steep uptakes at low relative pressures, corresponding to the presence of microporous features (d < 2 nm) and hysteresis at relative pressures >0.4 (Figure S6), indicating the presence of mesopores. Using the Brunauer−Emmett−Teller (BET) method,[29] the apparent specific surface areas are calculated to be 609, 942, 1500, and 2369 $m^2\ g^{-1}$ for SU-MC, SU-MAC-500, SU-MAC-600, and SU-MAC-800, respectively (Figures S7−10). It can be observed that higher activation temperatures gave rise to higher specific surface areas and larger pore volumes. This is attributed to the enhanced KOH activation reactions at higher temperatures. Note that the activation process led to shrinkage of the original mesopore distribution of SU-MC (Figure S11), which indicates the thermal instability of the mesostructure under the oxidative activation conditions. Besides, it can also be observed that KOH activation at elevated temperatures created additional pore volumes in the range of 0.7−5 nm (Figure 2f). Note that SU-MAC-500 possesses an ultramicropore (d < 0.7 nm)

DOI: 10.1021/jacs.5b11955
J. Am. Chem. Soc. 2016, 138, 1001−1009

Table 1. Summary of Textual Properties and CO_2 Capture Performances of SU-MAC Materials in Comparison to Literature Reported Physisorptive Nitrogen-Doped Carbons with Either the Highest Capacity or the Highest Selectivity[a]

		properties				CO_2 capacity at 298 K (mmol g^{-1})		selectivity		
material	activation	BET SSA[b] (m^2 g^{-1})	V_{micro}[c] (cm^3 g^{-1})	$V_{ultramicro}$[d] (cm^3 g^{-1})	N wt %	0.1 bar	1 bar	Henry's law CO_2/N_2[e]	IAST CO_2/N_2[f]	ref
MCN/C	no	338	0.06	–	24.9	0.7	2.4	–	40:1	47
HCM_DAH-1	no	670	0.20	–	4.1	0.7	2.6	28:1	30:1	46
H-NMC-2.5	no	537	0.17	–	13.1	1.0	2.8	37:1	35:1	48
RFL-500	no	467	0.21	–	1.9	0.9	3.1	–	29:1	49
nZDC-700	no	950	0.35	–	–	1.1	3.5	–	76:1	50
NPC-2	yes	1255.9	0.52	–	5.21	1.05	4.02	–	32:1	51
NC-650-1	yes	1483	0.57	0.61 (<1 nm)	4.56	1	4.26	29:1	23:1	52
CN-950		1979	–	–	4.32	1.4	4.3	30:1	12:1	53
a-NDC6	yes	1360	0.57	–	4.8	0.86	4.3	34:1	30:1	54
SNS2−20	yes	2100	0.93	0.35	–	1.6	4.48	–	36:1	45
CPC 550	yes	1630	0.59	0.35	7.88	1.48	5.8	59:1	21:1	33
SU-MAC-500	yes	941	0.34	0.30	5.8	1.42	4.50	124:1	39:1	this work
SU-MAC-600	yes	1500	0.50	0.27	4.0	0.82	4.18	32:1	22:1	this work
SU-MAC-800	yes	2369	0.63	0.18	3.2	0.40	3.11	9:1	11:1	this work

[a]Refer to Table S2 for a complete list of physisorptive micro- and mesoporous carbons. The entries are arranged with increased capacity at 1 bar. [b]BET specific surface area. [c]Cumulative micropore volume with diameter ≤ 2 nm. [d]Cumulative ultramicropore volume with diameter ≤ 0.7 nm. [e]Henry's Law selectivity at 298 K (see Supporting Information). [f]IAST selectivity at 298 K for the mixture of 0.1/0.9 CO_2/N_2 at 1 bar (see Supporting Information).

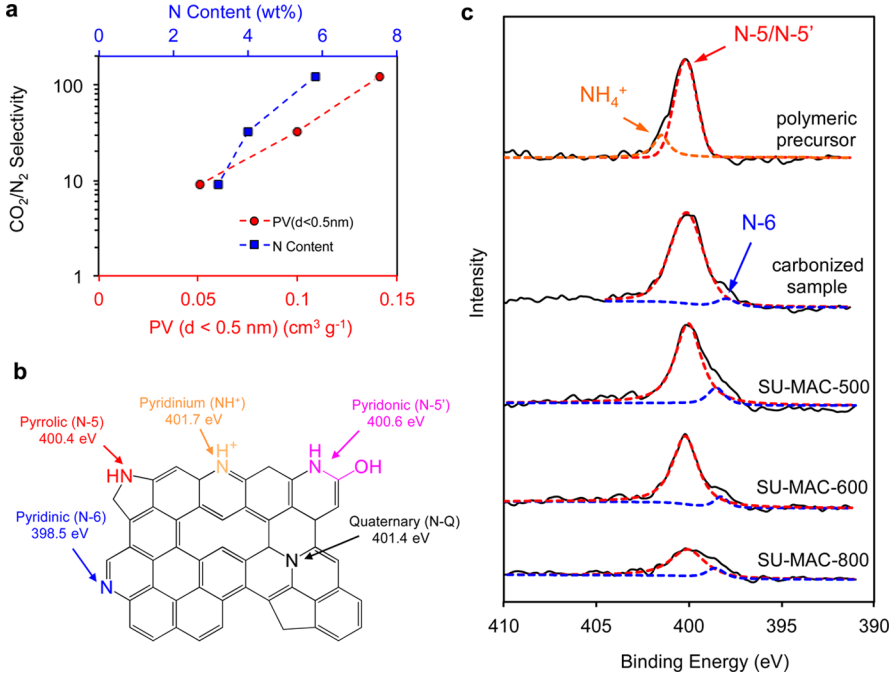

Figure 4. Selectivity correlations and chemical compositions of the hierarchical carbons. (a) Correlations between CO_2/N_2 selectivity and ultrasmall (d < 0.5 nm) pore volume and between CO_2/N_2 selectivity and N content. (b) Schematics of various types nitrogen functionalities including N-5/N-5′, N-6, N-Q, and NH_4^+. (c) XPS on N 1s (398.5 eV: N-6, 400.4−400.6 eV: N-5/N-5′, 401.4 eV: N-Q, 401.7 eV: NH_4^+).

volume of 0.30 cm^3 g^{-1}, which constitutes a remarkable 64% of its total pore volume (0.47 cm^3 g^{-1}).

CO_2 Capture Performance. At 298 K and 1 bar, SU-MAC-500 exhibited a high CO_2 adsorption capacity of 4.50 mmol g^{-1} (Figure 3a). The excellent CO_2 capacity of SU-MAC-500 is among the best of previously described physisorptive micro- and mesoporous carbons (Table S2). The CO_2/N_2 selectivity, acquired from Henry's law (see Supporting Information) is 124:1 at 298 K. This selectivity exceeds those of the literature nitrogen-doped carbons (Table 1) and other physisorptive carbons (Table S2). The selectivity was observed to increase as temperature increases (107:1 at 273 K; 194:1 at 323 K). Similar temperature dependencies were previously reported for a CO_2-philic mesoporous phenolic-functionalized melamine resin[30] and N_2-phobic nitrogen-rich azo-covalent organic polymers.[31] In addition, the ideal adsorption solution theory (IAST) selectivity (assuming 0.1/0.9 mixture of CO_2/N_2 at 1 bar) was found to be 27:1, 39:1, and 139:1 at 273, 298, and 323 K,

DOI: 10.1021/jacs.5b11955
J. Am. Chem. Soc. 2016, 138, 1001−1009

respectively (see Supporting Information). The discrepancy between the Henry's law and IAST values can be attributed to the adsorption site heterogeneity.[32] Figure 3b summarizes the capacity and Henry's law CO_2/N_2 selectivity of various types of solid physisorbents. Note that the amine-modified porous materials can potentially reach a higher CO_2/N_2 selectivity due to their chemical reactivity with CO_2,[6] which is not discussed here in detail. Although literature nitrogen-doped porous carbons reached maximum capacities (298 K) of 1.5 and 5.8 mmol g^{-1} at 0.1 and 1 bar, respectively, the selectivity remains to be low (i.e., 59 using Henry's law).[33] The additional functionalization step required for those chemisorptive carbons increases the cost of separation, and their long-term stability is yet to be determined.

The interaction strength between CO_2 and SU-MAC-500 was further evaluated by its isosteric heat of adsorption (Q_{st}) (Figure 3d). SU-MAC-500 shows a high Q_{st}, which ranges from 46 to 28 kJ mol^{-1} at CO_2 loadings of 0.01−2 mmol g^{-1}. The high Q_{st} at low CO_2 loading could be a result from the surface interactions between CO_2 and the basic nitrogen functionalities and/or enhanced fluid−fluid interactions of confined CO_2 in narrow pores.[34,35] The non-uniformity of Q_{st} over the entire range of CO_2 loadings suggests the adsorption site heterogeneity of the material. As the CO_2 loading increases, the adsorbed CO_2 molecules occupy the strong binding sites, therefore leaving the weaker binding sites available.

Effect of Sorbent's Pore Size and Structure. To better understand the reasons behind our observed high CO_2/N_2 selectivity, we investigated the effect of pore sizes and structures within the sorbent. From SU-MAC-500 to SU-MAC-800, the CO_2 adsorption at 298 K shows a decreasing trend as the activation temperature increases (Figure 3c, Table S3). The weakening in the CO_2−sorbent interactions over increasing activation temperatures is evidenced by the decrease in Q_{st} (Figure 3d). Again using Henry's law, the CO_2/N_2 selectivities for SU-MAC-600 and SU-MAC-800 were calculated to be 32:1 and 9:1, respectively (see Supporting Information). Note that the decreasing trend of CO_2/N_2 selectivity over the three SU-MAC samples is in good agreement with the trend of Q_{st}.

From structure characterization, it appears that neither the specific surface area nor the total pore volume directly contributes to the CO_2/N_2 selectivity. The microporous features can be observed from the CO_2 pore size distribution (PSD) (Figures 2f and S11). With increasing activation temperature the 0.35 and 0.48 nm peaks decrease in intensity, while the 0.58 and 0.8 nm peaks increase in intensity. This suggests that high-temperature activation creates an enhanced chemical etching effect on the carbon framework, creating additional volume of wider pores (0.58 and 0.8 nm) (Figure S11).

Interestingly, the trend of the CO_2/N_2 selectivity over the three SU-MAC samples is in agreement with that of cumulative volumes in the range of d < 0.5 nm (Figure 4a). Within these ultrasmall pores, the CO_2 adsorption potential energy is dramatically enhanced. Ultramicropores have been known to be important in CO_2 capture as they largely correspond with the CO_2 adsorption capacity in carbon materials.[21,22] This enhancement is caused by the superposition of the van der Waals force fields, which are strengthened by the narrowing of the adjacent pore walls.[39,40] The N_2 adsorption potential energy also increases, but to a much smaller extent. Therefore, the high abundance of ultrasmall pores within SU-MAC-500 (64% of its total pore volume) may be an important factor for its high CO_2/N_2 selectivity. The mild carbonization process, followed by low-temperature activation, allows the development of significant amounts of ultrasmall pores.

Effects of Sorbent Chemical Composition. To understand the sorbent's chemical composition, elemental analysis (EA) and X-ray photoelectron spectroscopy (XPS) were performed. The bulk nitrogen content was found to increase from 3.2 to 5.8 wt % with decreasing activation temperature (Table S4). This trend is consistent with previously reported literatures that high activation temperature caused degradation of nitrogen functional groups.[21,41] As shown in Figure 4a, the CO_2/N_2 selectivity increases with increasing nitrogen content of the materials, which indicate that the nitrogen functionalities could play an important role in the selectivity. The nature of the nitrogen species on the surface of carbon was further investigated using XPS characterization. Figure 4b illustrates the common nitrogen functionalities and their corresponding binding energies. The N 1s core level spectra of the as-synthesized polymer, carbonized SU-MC, and activated SU-MAC prepared at temperatures between 500 to 800 °C are shown in Figure 4c. As expected, the starting polymeric precursor, poly(4-(pyrrol-1-yl)butanoic acid), shows only one major peak at 400.5 eV, corresponding to the pyrrolic nitrogen (N-5),[42] with a very minor peak at 401.7 eV, probably due to the formation of protonated nitrogen under the acidic synthetic condition. When the polymer is carbonized, the minor peak disappears, while an additional small shoulder peak at 398.8 eV appears, corresponding to the pyridinic nitrogen (N-6). After chemical activation, the two peaks continue to exist at 398.8 and 400.6 eV. However, given the oxidative conditions of the chemical activation process, the nitrogen found at this oxidative condition could potentially be pyridonic N-5′, which has a similar binding energy (400.4−400.6 eV) as pyrrolic N-5. The same observation and assignment were reported in previous literature and both pyrrolic and pyridonic N-5′ have been suggested to have stronger interactions with CO_2 gas molecules.[34,43] It is interesting to note that the ratio of N-5′:N-6 decreased with increased activation temperature (Table S4). This is caused by a rearrangement in the C−N bond to a more thermodynamically stable state (N-6) under elevated temperature.[41] Therefore, in SU-MAC-500, pyrrolic/pyridonic N-5 are the dominant nitrogen species (86.8%), along with 13.2% pyridinic nitrogen (N-6). It is also interesting to note that nitrogen species tends to leave the carbon framework forming gaseous product under oxidizing environment (KOH activation) via the formation of an epoxy intermediate.[44] This finding is consistent with the increased CO_2 selectivity and the Q_{st} in the activated samples. Furthermore, the residue potassium cation K^+ (ca. 1% in SU-MAC-500) can possibly contribute to the high selectivity. Kim et al. showed that with impregnation of a highly basic reagent, CO_2 capacity could be enhanced due to the strengthened interaction between the acidic CO_2 and the basic component in the carbon framework.[45] To further elucidate the existence of such strong adsorption site within the carbon framework, we calculated a virial plot of CO_2 adsorption (Figure S17). Highly nonlinearity is observed with a "dip" at the low uptake range, suggesting the presence of numerous strong sites.[32] At low pressures, CO_2 preferentially interacts with the strong sites, causing the dip in the virial plot; whereas at high pressures, the plot is flattened out and becomes linear, which means CO_2 gas molecules are occupying the weaker adsorption sites.

DOI: 10.1021/jacs.5b11955
J. Am. Chem. Soc. 2016, 138, 1001−1009

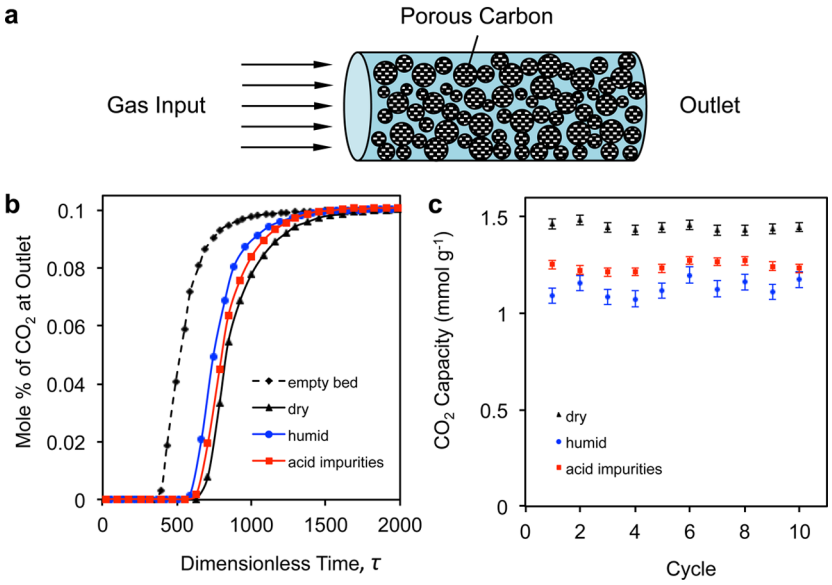

Figure 5. CO_2 adsorption tested under various conditions. (a) Schematic of a packed-bed adsorption column. (b) CO_2 mole faction profiles detected at the outlet of the adsorption column for empty bed and SU-MAC-500 with a mixed gas input of 10%/90% CO_2/N_2 at 298 K and total pressure of 1 bar. Operating conditions include dry, humid, or with acid impurities (dimensionless time: $\tau = tu/\varepsilon L$). The dynamic CO_2 capacity was calculated by the CO_2 mass balance based upon the integration of the CO_2 breakthrough curves subtracted by that of a blank experiment.[32] (c) Multicycle dynamic column CO_2 adsorption capacity (298 K) of SU-MAC-500 at a CO_2 partial pressure of 0.1 bar with balance N_2 under different conditions: dry, humid, or with acid impurities.

Realistic CO_2 Adsorption and Cycling Stability Performance. To assess the potential of applying the sorbent in practical processes, more realistic conditions are required, i.e., competitive CO_2 adsorption with N_2 in a dynamic system. Furthermore, regenerability and stability over multiple cycles are critical requirements for practical applications. Figure 5a shows a schematic of a packed-bed adsorption column. In a typical experiment, a mixed gas stream of 10% (v/v) CO_2 + 90% (v/v) N_2 was used to approximately simulate a postcombustion flue gas (Figure S18). At 298 K and 0.1 bar partial pressure of CO_2, the dynamic CO_2 capacity of SU-MAC-500 is 1.45 ± 0.03 mmol g^{-1}, which matches well with that from the equilibrium measurements using pure CO_2 at 298 K and 0.1 bar, i.e., 1.42 ± 0.04 mmol g^{-1}. This implies that CO_2 still preferentially adsorbs onto the sorbent material over N_2, even in a CO_2/N_2 mixture.

Furthermore, reversibility of CO_2 adsorption was tested by the dynamic column breakthrough method.[32] To a sample saturated with CO_2, pure N_2 was purged at 298 K until no CO_2 was detected from the effluent. Subsequent CO_2 adsorption suggests full recovery of the CO_2 capacity. Further, the dynamic CO_2 capacity of SU-MAC-500 under humid conditions (~3 vol % water, 0.1 bar CO_2, 298 K) was found to be as high as 1.13 ± 0.04 mmol g^{-1}, corresponding only a 22% decrease compared to the dry CO_2 capacities. While there is limited data available under humid conditions for CO_2 physisorption onto porous carbons, the humid CO_2 capacity of SU-MAC-500 exceeds that of a previously reported nitrogen-containing mesoporous carbon, i.e., 0.91 mmol g^{-1}, with an even slightly higher CO_2 partial pressure (0.14 bar).[46] In addition, the dynamic column breakthrough was also conducted at a higher temperature of 323 K with capacities of 0.71 ± 0.03 and 0.54 ± 0.03 mmol g^{-1} under dry and humid conditions, respectively (Figure S19).

To investigate the sorbent performance under more realistic conditions, a simulated flue gas generated from burning bituminous coal was tested. More specifically, the following trace amounts of acid impurities were introduced into the 10%/90% CO_2/N_2 mixture: 200 ppm of SO_2, 100 ppm of NO, and 5 ppm of NO_2. The CO_2 capacity was maintained at a high level of 1.24 ± 0.03 mmol g^{-1}, corresponding to a 14% decrease compared to the pure CO_2 capacity. Figure 5b shows CO_2 breakthrough profiles, where it was observed that the breakthrough curves for the humid and acidic conditions were shifted to earlier times as compared to the dry test, corresponding to a reduction of CO_2 adsorption capacity. There is a lack in the literature on the impact of acidic impurities on the CO_2 adsorption onto physisorptive carbons. It should be noted that the slope of the sorbent breakthrough curves under all tested conditions resembles that of the blank breakthrough curve, which means the CO_2 gas adsorbed instantaneously upon contact with the sorbent, i.e., fast gas diffusion and adsorption.[32] Ten cycles of adsorption and desorption were performed on SU-MAC-500 under dry, humid, or acid impurity conditions without loss of CO_2 capacities at all conditions (Figure 5c). Hence, SU-MAC-500 can be fully regenerated over multiple cycles.

■ CONCLUSIONS

In conclusion, we have demonstrated a novel hierarchical N-doped carbon prepared by rational design of a modified pyrrole monomer that enables co-assembly with the soft triblock copolymer template via hydrogen bonding and electrostatic interactions. Subsequently, low-temperature carbonization and activation processes of the conjugated polymer framework lead to abundant ultrasmall pores and strong CO_2 binding nitrogen sites, which are essential in enhancing the CO_2-sorbent interactions and selectivity. The resulting hierarchical porous carbon achieved a record-high Henry's law CO_2/N_2 selectivity of 124:1 at ambient temperature among previously reported physisorptive carbons. This carbon can be fully regenerated under mild conditions and exhibited high performance and excellent stability under humid conditions or circumstances

DOI: 10.1021/jacs.5b11955
J. Am. Chem. Soc. 2016, 138, 1001−1009

with acid impurities. This work for the first time presents CO_2 adsorption tests with acid impurities on nitrogen-doped physisorptive carbons. The described work provides a strategy to initiate further development of promising conjugated polymer- and carbon-based sorbents.

EXPERIMENTAL SECTION

Materials. All chemicals and solvents were purchased from Sigma-Aldrich and used without further purification. 4-(pyrrol-1-yl)butanoic acid is synthesized according to previous work (see Supporting Information).

Synthesis of Nitrogen-Doped Mesoporous Polymer/Mesoporous Carbon (SU-MC). Triblock copolymer Pluronic P-123 is used as the soft-template for the synthesis of mesoporous polypyrrole. Hydrochloric acid and an ice water bath were used to control the solution pH and temperature, respectively. Ferric chloride ($FeCl_3$) was added to the aqueous solution to polymerize 4-(pyrrol-1-yl)butanoic acid co-assembled with the soft-template surfactant in a controlled manner as described below.

In a typical synthesis, Pluronic P-123 (0.598 g, purchased from Aldrich and used as received) and ferric chloride (1.14 g) were added to a mixture of Millipore water (15 mL) and 12 M HCl solution (2.5 mL) cooled with an ice water bath. The solution was vigorously mixed for 2 h before 4-(pyrrol-1-yl)butanoic acid was added dropwise to the above solution. After vigorous stirring with a magnetic stirring bar for 20 min in air, this solution was allowed to sit without stirring in an ice water bath for 20 h, followed by hydrothermal heating to 100 °C to complete the polymerization of the 4-(pyrrol-1-yl)butanoic acid monomers. The hydrothermal product was then filtered and washed with deionized water repeatedly. Carbonization was performed in a horizontal tube furnace (25 mm diameter) under N_2 (99.999%) flow of 75 sccm and a working pressure of ~520 Torr. The polymer composite was first heated to 350 °C at a ramp rate of 1 °C/min and held for 3 h to slowly decompose the triblock copolymer surfactant, followed by heating to 600 °C at a ramp rate of 1 °C/min and finally to 800 °C with 5 °C/min and held for 2 h to produce the porous carbon (SU-MC) with a yield of 35%. Additionally, we found that lowering the temperature to 0 °C during oxidative polymerization can slow down the pyrrole polymerization process, thereby helping to maintain the mesostructure and in avoiding polymer−polymer demixing.[24]

Synthesis of Nitrogen-Doped Hierarchical Activated Carbon (SU-MAC). Oxidative chemical activation of a low-temperature carbonized sample of SU-MC using potassium hydroxide (KOH) was performed to generate SU-MAC. In a standard procedure, the as-synthesized poly(4-(pyrrol-1-yl)butanoic acid) composite was carbonized in a horizontal tube furnace under N_2 flow to 350 °C at a ramp rate of 1 °C/min and hold for 3 h, denoted here as SU-MC-350. The powder was collected and dispersed in a 7 M aqueous KOH solution using a mass ratio of 3:1 for KOH to SU-MC-350. The mixture was stirred for 2 h and dried in vacuum oven at 65 °C for 4 h, which is then followed by heating under N_2 to 500 °C (ramping rate: 5 °C·min^{-1}, holding time: 1 h). The activated samples were then thoroughly washed three times with HCl solution (10 wt %) to remove any remaining inorganic salts and then washed extensively with deionized water until a neutral pH was measured. Finally, the activated carbon was dried in an oven at 65 °C in vacuum oven overnight. The nitrogen-doped hierarchical activated carbons thus synthesized are denoted as SU-MAC-500, with an overall yield of 21%. Those activated at 600 and 800 °C are denoted as SU-MAC-600 and SU-MAC-800, respectively.

Characterization. SEM was performed using an FEI Magellan 400 XHR microscope with a 5 kV accelerating voltage and 25 pA current. TEM investigations were performed using a 200 kV TEM FEI Tecnai T20 instrument. The elemental composition of the surfaces was measured with XPS (PHI 5000 Versaprobe, Al KR source). Elemental analysis was performed using a Carlo-Erba NA 1500 analyzer for determination of total nitrogen and carbon content of the bulk samples. ^{1}H NMR spectrum was recorded using Varian Inova 500 in deuterated chloroform at 293 K. TG analysis was carried out using a Mettler Toledo TGA- sDTA851 analyzer (Switzerland) from 25 to 800 °C under nitrogen a heating rate of 5 °C min^{-1}. N_2 and CO_2 sorption experiments were performed using an Autosorb iQ$_2$ (Quantachrome) low-pressure gas sorption analyzer. The samples were outgassed at 0.001 Torr and 200 °C for 12 h prior to measurements. N_2 physisorption analysis was carried out using 99.999% N_2 at 77 K. The N_2 PSD was obtained using a nonlocal density functional theory (NLDFT) carbon model with slit and cylindrical geometries. Specific surface areas were obtained by the BET method. The same outgassing procedure was adapted for the CO_2 adsorption measurements. CO_2 adsorption was performed at 273, 298, and 323 K with the temperature controlled using a circulating bath. The CO_2 PSD was calculated using the NLDFT carbon model based upon the CO_2 adsorption isotherm at 273 K. All measurements have been repeated three times, and the average values are reported.

Dynamic Column Breakthrough Experiments. See Supporting Information.

ASSOCIATED CONTENT

Supporting Information

The Supporting Information is available free of charge on the ACS Publications website at DOI: 10.1021/jacs.5b11955.

Materials preparation; dynamic column breakthrough experiments and setup; density measurements; small-angle XRD results; BET calculations and fittings; PSDs of all samples; selectivity calculation using Henry's law method and IAST; ^{1}H NMR spectrum of 4-(pyrrol-1-yl)butanoic acid (PDF)

AUTHOR INFORMATION

Corresponding Authors

*wilcoxj@stanford.edu

*zbao@stanford.edu

Author Contributions

⊥These authors contributed equally.

Notes

The authors declare no competing financial interest.

ACKNOWLEDGMENTS

This work is partially supported by the Global Climate and Energy Program (GCEP), Stanford Precourt Institute for Energy, and the SUNCAT Center for Interfaces and Catalysis, a partnership between SLAC National Accelerator Laboratory and the Department of Chemical Engineering at Stanford University. J.W.F.T. acknowledges the support from the Croucher Foundation.

REFERENCES

(1) *Climate Change 2007: Synthesis Report*; Intergovernmental Panel on Climate Change (IPCC): Geneva, Switzerland, 2007.

(2) Chen, Z. H.; Deng, S. B.; Wei, H. R.; Wang, B.; Huang, J.; Yu, G. *Front. Environ. Sci. Eng.* **2013**, *7*, 326.

(3) D'alessandro, D. M.; Smit, B.; Long, J. R. *Angew. Chem., Int. Ed.* **2010**, *49*, 6058.

(4) Xu, F.; Tang, Z. W.; Huang, S. Q.; Chen, L. Y.; Liang, Y. R.; Mai, W. C.; Zhong, H.; Fu, R. W.; Wu, D. C. *Nat. Commun.* **2015**, *6*, 7221.

(5) Dai, L. M.; Xue, Y. H.; Qu, L. T.; Choi, H. J.; Baek, J. B. *Chem. Rev.* **2015**, *115*, 4823.

(6) Choi, S.; Drese, J. H.; Jones, C. W. *ChemSusChem* **2009**, *2*, 796.

(7) To, J. W. F.; Chen, Z.; Yao, H.; He, J.; Kim, K.; Chou, H.-H.; Pan, L.; Wilcox, J.; Cui, Y.; Bao, Z. *ACS Cent. Sci.* **2015**, *1*, 68.

(8) Wan, Y.; Shi, Y.; Zhao, D. *Chem. Mater.* **2008**, *20*, 932.

(9) Epps, T. H.; Cochran, E. W.; Hardy, C. M.; Bailey, T. S.; Waletzko, R. S.; Bates, F. S. *Macromolecules* **2004**, *37*, 7085.

DOI: 10.1021/jacs.5b11955
J. Am. Chem. Soc. 2016, 138, 1001−1009

(10) Wu, Z.; Zhao, D. *Chem. Commun.* **2011**, *47*, 3332.
(11) Nugent, P.; Belmabkhout, Y.; Burd, S. D.; Cairns, A. J.; Luebke, R.; Forrest, K.; Pham, T.; Ma, S. Q.; Space, B.; Wojtas, L.; Eddaoudi, M.; Zaworotko, M. J. *Nature* **2013**, *495*, 80.
(12) Meng, Y.; Gu, D.; Zhang, F. Q.; Shi, Y. F.; Yang, H. F.; Li, Z.; Yu, C. Z.; Tu, B.; Zhao, D. Y. *Angew. Chem., Int. Ed.* **2005**, *44*, 7053.
(13) Zhang, F. Q.; Meng, Y.; Gu, D.; Yan, Y.; Yu, C. Z.; Tu, B.; Zhao, D. Y. *J. Am. Chem. Soc.* **2005**, *127*, 13508.
(14) Feng, D.; Lv, Y. Y.; Wu, Z. X.; Dou, Y. Q.; Han, L.; Sun, Z. K.; Xia, Y. Y.; Zheng, G. F.; Zhao, D. Y. *J. Am. Chem. Soc.* **2011**, *133*, 15148.
(15) Fang, Y.; Lv, Y. Y.; Che, R. C.; Wu, H. Y.; Zhang, X. H.; Gu, D.; Zheng, G. F.; Zhao, D. Y. *J. Am. Chem. Soc.* **2013**, *135*, 1524.
(16) Liu, J.; Yang, T. Y.; Wang, D. W.; Lu, G. Q. M.; Zhao, D. Y.; Qiao, S. Z. *Nat. Commun.* **2013**, *4*, 2798.
(17) Liang, C.; Hong, K.; Guiochon, G. A.; Mays, J. W.; Dai, S. *Angew. Chem., Int. Ed.* **2004**, *43*, 5785.
(18) Liang, C.; Li, Z.; Dai, S. *Angew. Chem., Int. Ed.* **2008**, *47*, 3696.
(19) Ho, M. T.; Allinson, G. W.; Wiley, D. E. *Ind. Eng. Chem. Res.* **2008**, *47*, 4883.
(20) Pirngruber, G. D.; Leinekugel-le-Cocq, D. *Ind. Eng. Chem. Res.* **2013**, *52*, 5985.
(21) Sevilla, M.; Parra, J. B.; Fuertes, A. B. *ACS Appl. Mater. Interfaces* **2013**, *5*, 6360.
(22) Presser, V.; McDonough, J.; Yeon, S. H.; Gogotsi, Y. *Energy Environ. Sci.* **2011**, *4*, 3059.
(23) Lipic, P. M.; Bates, F. S.; Hillmyer, M. A. *J. Am. Chem. Soc.* **1998**, *120*, 8963.
(24) Li, D.; Huang, J.; Kaner, R. B. *Acc. Chem. Res.* **2009**, *42*, 135.
(25) Liao, Y.; Li, X.-G.; Kaner, R. B. *ACS Nano* **2010**, *4*, 5193.
(26) Pan, L.; Pu, L.; Shi, Y.; Sun, T.; Zhang, R.; Zheng, Y. *Adv. Funct. Mater.* **2006**, *16*, 1279.
(27) Dugas, V.; Chevalier, Y. *Langmuir* **2011**, *27*, 14188.
(28) Stejskal, J.; Sapurina, I.; Trchová, M.; Konyushenko, E. N.; Holler, P. *Polymer* **2006**, *47*, 8253.
(29) Brunauer, S.; Emmett, P. H.; Teller, E. *J. Am. Chem. Soc.* **1938**, *60*, 309.
(30) Lee, J. H.; Lee, H. J.; Lim, S. Y.; Kim, B. G.; Choi, J. W. *J. Am. Chem. Soc.* **2015**, *137*, 7210.
(31) Patel, H. A.; Hyun Je, S.; Park, J.; Chen, D. P.; Jung, Y.; Yavuz, C. T.; Coskun, A. *Nat. Commun.* **2013**, *4*, 1357.
(32) Ruthven, D. M. *Principles of adsorption and adsorption processes*; John Wiley & Sons: Hoboken, NJ, 1984.
(33) Ashourirad, B.; Sekizkardes, A. K.; Altarawneh, S.; El-Kaderi, H. M. *Chem. Mater.* **2015**, *27*, 1349.
(34) Sevilla, M.; Valle-Vigon, P.; Fuertes, A. B. *Adv. Funct. Mater.* **2011**, *21*, 2781.
(35) Jin, Y. G.; Hawkins, S. C.; Huynh, C. P.; Su, S. *Energy Environ. Sci.* **2013**, *6*, 2591.
(36) Huang, N.; Chen, X.; Krishna, R.; Jiang, D. L. *Angew. Chem., Int. Ed.* **2015**, *54*, 2986.
(37) Xiang, S. C.; He, Y. B.; Zhang, Z. J.; Wu, H.; Zhou, W.; Krishna, R.; Chen, B. L. *Nat. Commun.* **2012**, *3*, 954.
(38) DeCoste, J. B.; Peterson, G. W.; Schindler, B. J.; Killops, K. L.; Browe, M. A.; Mahle, J. J. *J. Mater. Chem. A* **2013**, *1*, 11922.
(39) Everett, D. H.; Powl, J. C. *J. Chem. Soc., Faraday Trans. 1* **1976**, *72*, 619.
(40) Cui, X.; Bustin, R. M.; Dipple, G. *Fuel* **2004**, *83*, 293.
(41) Pels, J.; Kapteijn, F.; Moulijn, J.; Zhu, Q.; Thomas, K. *Carbon* **1995**, *33*, 1641.
(42) Gammon, W.; Kraft, O.; Reilly, A.; Holloway, B. *Carbon* **2003**, *41*, 1917.
(43) Gracia, S.; Cazorla, C.; Métay, E.; Pellet-Rostaing, S.; Lemaire, M. *J. Org. Chem.* **2009**, *74*, 3160.
(44) Stöhr, B.; Boehm, H. P.; Schlögl, R. *Carbon* **1991**, *29*, 707.
(45) Kim, Y. K.; Kim, G. M.; Lee, J. W. *J. Mater. Chem. A* **2015**, *3*, 10919.
(46) Hao, G.-P.; Li, W.-C.; Qian, D.; Wang, G.-H.; Zhang, W.-P.; Zhang, T.; Wang, A.-Q.; Schüth, F.; Bongard, H.-J.; Lu, A.-H. *J. Am. Chem. Soc.* **2011**, *133*, 11378.
(47) Deng, Q.-F.; Liu, L.; Lin, X.-Z.; Du, G.; Liu, Y.; Yuan, Z.-Y. *Chem. Eng. J.* **2012**, *203*, 63.
(48) Wei, J.; Zhou, D.; Sun, Z.; Deng, Y.; Xia, Y.; Zhao, D. *Adv. Funct. Mater.* **2013**, *23*, 2322.
(49) Hao, G.-P.; Li, W.-C.; Qian, D.; Lu, A.-H. *Adv. Mater.* **2010**, *22*, 853.
(50) Gadipelli, S.; Guo, Z. X. *ChemSusChem* **2015**, *8*, 2123.
(51) Wan, L.; Wang, J. L.; Feng, C.; Sun, Y. H.; Li, K. X. *Nanoscale* **2015**, *7*, 6534.
(52) Yang, M. L.; Guo, L. P.; Hu, G. S.; Hu, X.; Xu, L. Q.; Chen, J.; Dai, W.; Fan, M. H. *Environ. Sci. Technol.* **2015**, *49*, 7063.
(53) Ma, X. Y.; Cao, M. H.; Hu, C. W. *J. Mater. Chem. A* **2013**, *1*, 913.
(54) Chandra, V.; Yu, S. U.; Kim, S. H.; Yoon, Y. S.; Kim, D. Y.; Kwon, A. H.; Meyyappan, M.; Kim, K. S. *Chem. Commun.* **2012**, *48*, 735.

DOI: 10.1021/jacs.5b11955
J. Am. Chem. Soc. 2016, 138, 1001−1009